ACS Catalysis

RESEARCH ARTICLE

pubs.acs.org/acscatalysis

# Anthracene-Modified Multi-Walled Carbon Nanotubes as Direct Electron Transfer Scaffolds for Enzymatic Oxygen Reduction

Matthew T. Meredith,[†] Michael Minson,[†] David Hickey,[‡] Kateryna Artyushkova,[§] Daniel T. Glatzhofer,[‡] and Shelley D. Minteer*[,†]

[†]Department of Chemistry, University of Utah, Salt Lake City, Utah 84112, United States

[‡]Department of Chemistry and Biochemistry, University of Oklahoma, Norman, Oklahoma 73019, United States

[§]Department of Chemical & Nuclear Engineering, Center for Emerging Energy Technologies, University of New Mexico, Albuquerque, New Mexico 87131, United States

Supporting Information

**ABSTRACT:** The development of new methods to facilitate direct electron transfer (DET) between enzymes and electrodes is of much interest because of the desire for stable biofuel cells that produce significant amounts of power. In this study, hydroxylated multiwalled carbon nanotubes (MWCNTs) were covalently modified with anthracene groups to help orient the active sites of laccase to allow for DET. The onset of the catalytic oxygen reduction current for these biocathodes occurred near the potential of the T1 active site of laccase, and optimized biocathodes produced background-subtracted current densities up to 140 $\mu$A/cm$^2$. Potentiostatic and galvanostatic stability measurements of the biocathodes revealed losses of 25% and 30%, respectively, after 24 h of constant operation. Finally, the novel biocathodes were utilized in biofuel cells employing two different anodic enzymes. A compartmentalized cell using a mediated glucose oxidase anode produced an open circuit voltage of 0.819 ± 0.022 V, a maximum power density of 56.8 (±1.8) $\mu$W/cm$^2$, and a maximum current density of 205.7 (±7.8) $\mu$A/cm$^2$. A compartment-less cell using a DET fructose dehydrogenase anode produced an open circuit voltage of 0.707 ± 0.005 V, a maximum power density of 34.4 (±2.7) $\mu$W/cm$^2$, and a maximum current density of 201.7 (±14.4) $\mu$A/cm$^2$.

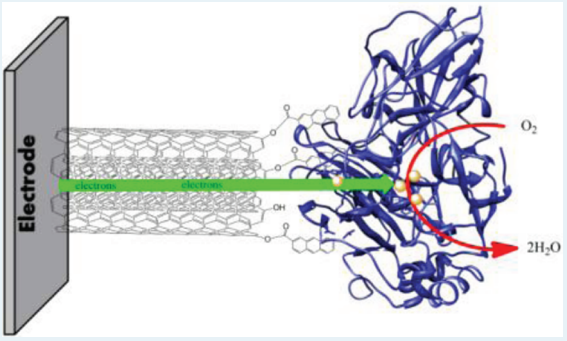


**KEYWORDS:** bioelectrocatalysis, laccase, anthracene, direct electron transfer, oxygen reduction reaction

## INTRODUCTION

The field of bioelectrocatalysis has flourished recently because of the growing interest in producing electrical energy from biologically renewable resources. Enzymatic biofuel cells are one type of device that can produce this renewable energy, and much research has been focused on engineering modified electrode surfaces that allow for the electrical connection of enzyme active sites to electrodes.[1−4] Two primary methods are used for this connection: mediated electron transfer (MET) and direct electron transfer (DET). In a mediated system, electrochemically reversible redox species are used to transport electrons between enzymes and metallic electrodes. MET systems typically involve the use of a polymer matrix that is used to immobilize the enzyme near the electrode surface, while the mediator can be dissolved in solution,[5−7] tethered to the immobilization polymer,[8−13] or immobilized in a separate layer on the electrode surface.[14−16] While MET systems can produce high current densities and allow for the connection of many layers of enzyme to an electrode surface, the presence of a mediator adds an additional source of instability and introduces activation loss, or overpotential that is necessary to overcome before bioelectrocatalysis can begin.[17]

To remove mediators from bioelectrocatalytic systems and still produce significant amounts of current and power, it is necessary to fabricate modified electrodes that directly connect the active sites of enzymes to the electrode surface. Some enzymes, such as glucose oxidase (GOx) have active sites which are buried deep within the protein shell,[18] which makes DET difficult. Other enzymes contain heme groups[19−21] or coordinated metal atoms[22−24] near to the enzyme surface which make DET possible because of short electron transfer distances between these sites and electrode surfaces. However, immobilizing an enzyme that *can* undergo DET onto an electrode does not mean that it *will* undergo DET with said electrode. The active site of the enzyme still needs to be near enough to the surface of the electrode for electron transfer to take place at a considerable rate.[25]

**Received:** September 16, 2011
**Revised:** October 7, 2011
**Published:** October 21, 2011

In addition, a significant number of the enzymes that are loaded onto the electrode need to achieve this orientation to produce a significant current.

One method for achieving significant DET current densities involves the mixing or encapsulation of enzymes within high surface area nanomaterials or coating them onto high surface-area electrodes to provide a highly conductive matrix that surrounds the enzymes.[26−30] Even though enzymes are randomly oriented in these electrodes, many of the active sites are oriented near enough to the conductive matrix to produce significant currents. These methods have recently been used to create biocathodes and bioanodes with extremely high current densities (above 1 mA/cm$^2$) using laccase as a cathodic enzyme and either fructose dehydrogenase (FDH)[30] or glucose oxidase[31] as an anodic enzyme. In one case, nanotube/enzyme composites were fabricated by the liquid-induced shrinkage of carbon nanotube forests around the enzymes,[30] and in the other case, enzyme/nanotube mixtures were simply compressed into electrode pellets that produced extremely high currents.[31] Modified carbon nanotubes have also been used by Tasca et al. to produce high DET currents using adsorbed cellobiose dehydrogenase as an anodic enzyme.[21] High surface area carbon nanoparticles have also been used as a scaffold for laccase and FDH adsorption to produce biofuel cells with maximum current densities near 1 mA/cm$^2$.[32] These examples show that under the right conditions, enzymes can be mixed with or adsorbed onto conductive nanomaterials to fabricate high performance biofuel cells.

A second method for achieving DET involves fabricating a modified electrode that allows for the strategic attachment of the enzyme nearer to the conductive matrix or electrode surface. This attachment can be covalent[33,34] or noncovalent,[35−37] with the goal of increasing the likelihood that enzyme active sites will be oriented near the conductive surface or matrix. Multicopper oxidases (MCOs) such as laccase and bilirubin oxidase (BOD) have been covalently linked to gold surfaces,[38] graphite,[39] and carbon nanotubes[33,40] to achieve DET. However, because covalent modification of enzymes can lower their activity, the noncovalent orientation of enzymes near electrode surfaces is desirable. Of note is the work of Armstrong et al., who have showed that the covalent modification of electrode surfaces with different aromatic groups leads to significantly enhanced electrocatalytic reduction of oxygen by the enzymes laccase and bilirubin oxidase,[36,37,41] part of the family of MCOs that can reduce oxygen to water at high potentials. They propose that the presence of aromatic moieties on electrode surfaces mimics the natural phenolic substrates of laccase and BOD and creates docking sites for the hydrophobic pocket that surrounds their active sites. This hypothesis has been further strengthened by the noncovalent attachment of laccase to anthracene-modified gold electrodes.[35]

On the basis of this aromatic docking methodology for MCOs and previous work in mixing enzymes with carbon nanotubes, we hypothesized that multiwalled carbon nanotubes (MWCNTs) could be modified with hydrophobic aromatic groups to favorably orient the active sites of laccase enzymes nearer to the surface of the highly conductive MWCNTs. This allows for the combination of two methodologies for DET enzyme immobilization and instead of the favorable orientation of only one layer of enzyme on an aromatically modified surface, this method should allow the enzyme to be intimately mixed with an aromatically modified conductive material and allow for the electrical wiring of many layers of enzymes. This report details our investigation into the synthesis of anthracene-modified MWCNTs, their use as catalysts for laccase-based DET biocathodes, and the use of said biocathodes in two different types of enzymatic biofuel cells.

## EXPERIMENTAL SECTION

**Chemicals and Solutions.** Laccase from *Trametes versicolor*, glucose oxidase from *Aspergillus niger* (EC 1.1.3.4, type X-S, 157 units/mg of solid, 75% protein), oxalyl chloride, glucose, fructose, Nafion EW1100 suspension, and all solvents and salts were purchased from Sigma-Aldrich and used as received. Fructose dehydrogenase from *Gluconobacter sp.* was purchased from Toyobo Enzymes and used as received. 2-Anthracenecarboxylic acid was purchased from TCI chemicals and used as received. Ethylene glycol diglycidyl ether (EGDGE) was purchased from Polysciences Inc., Warrington, PA, and used as received. Hydroxylated MWCNTs (10−30 $\mu$m length, 1.6% −OH functionalization) were purchased from cheaptubes.com and used as received. Stock solutions of glucose were allowed to mutarotate 24 h before use and were stored at 4 °C. The redox polymer $FcMe_2$-$C_3$-LPEI was synthesized as previously reported.[11] Tetrabutylammonium bromide (TBAB)-modified Nafion was also prepared as previously reported.[42]

**Anthracene-Modified MWCNTs.** Anthracene-2-carbonyl chloride was synthesized similar to previously published procedures[43,44] as follows: 2-anthracenecarboxylic acid (2.0 g) was dissolved in 30 mL of benzene, and 2.6 g (2.4 equiv) of oxalyl chloride was added dropwise. The mixture was stirred and heated to reflux solvent for 16 h under argon. The benzene and excess oxalyl chloride were removed under reduced pressure, and the product was rinsed with cold benzene to remove any residual oxalyl chloride, dried under argon, and used without any further purification (2.06 g of a bright yellow solid, 95.3% yield).

To modify the MWCNTs, 0.471 g of hydroxylated MWCNTs was added to 100 mL of acetonitrile and sonicated for 15 min. Anthracene-2-carbonyl chloride (0.372 g, containing 1.0 equiv of −OH groups) was added, and the mixture was stirred vigorously and heated to reflux solvent overnight. After the mixture cooled, the nanotubes were filtered out of solution and washed with copious amounts of acetonitrile, benzene, and dichlormethane to remove any unreacted anthracenes to produce 0.619 g of anthracene-modified MWCNTs (83.7% yield).

**UV−vis Spectroscopy.** UV−vis spectroscopy was carried out using a Hitachi U-4100 UV−visible-NIR Spectrophotometer in quartz cuvettes (1 cm path length) using dimethylformamide (DMF) as a solvent. Dilutions of 0.005 mg/mL (2-anthracenecarboxylic acid) and 0.001 mg/mL (unmodified/modified MWCNTs) were made in vials, sonicated for 5 min, and transferred to the cuvettes before use.

**X-ray Photoelectron Spectroscopy (XPS).** XPS spectra were acquired by a Kratos AXIS Ultra photoelectron spectrometer using a monochromatic Al K$\alpha$ source operating at 300 W. The base pressure was $2 \times 10^{-10}$ Torr, and operating pressure was $2 \times 10^{-9}$ Torr. Charge compensation was accomplished using low energy electrons. Standard operating conditions for good charge compensation are −4.1 V bias voltage, −1.0 V filament voltage, and a filament current of 2.1 A. The reported XPS data represent averages from 3 areas per sample. The survey of each area is done first, followed by the recording of high resolution spectra of C 1s and O 1s for all the samples. Au powder was put on each sample, and Au 4f spectra were acquired. Linear background was used for

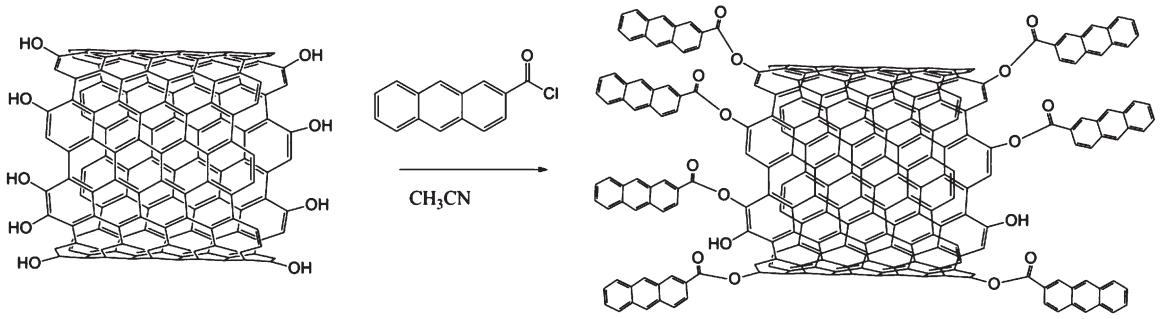


**Figure 1.** Covalent attachment of anthracene groups to MWCNTs.

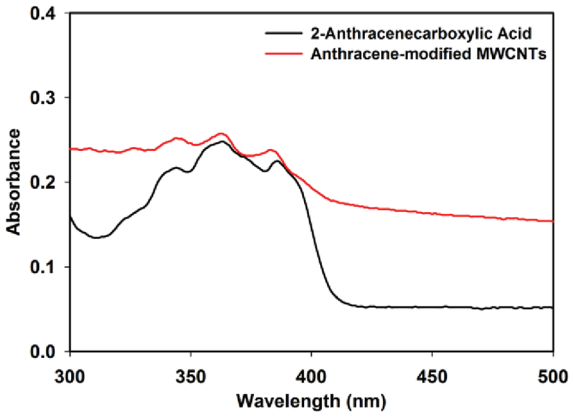


**Figure 2.** Absorption spectra of An-MWCNTs and 2-anthracenecarboxylic acid in DMF. A background of unmodified MWCNTs is subtracted from the spectrum of the An-MWCNTs to show the presence of the anthracene groups.

elemental quantification of C1s, and O1s spectra. Quantification utilized sensitivity factors provided by the manufacturer. All the spectra were charge referenced to the Au 4f at 84 eV. Curve fitting was carried out using individual peaks of constrained width, position, and 70% Gaussian/30% Lorentzian line shape.

**Enzyme Electrode Fabrication.** Biocathodes were fabricated as follows: laccase (3.0 mg) was dissolved in 150 $\mu$L of 100 mM phosphate buffer (pH 7.0), and 15.0 mg of anthracene-modified MWCNTs were added. This mixture was sonicated for 10 min and then briefly vortexed. To this mixture, 50 $\mu$L of TBAB-modified Nafion was added, and the mixture was briefly sonicated and vortexed again. The ink-like mixture was then painted onto 1 $cm^2$ pieces of Toray carbon paper with a small paintbrush and allowed to dry overnight at room temperature. In the optimization experiments, the amounts of laccase and anthracene-modified MWCTNs were changed accordingly, but the final volume of the casting solution was always 200 $\mu$L. Enzyme electrode casting solutions for the glucose oxidase bioanodes were prepared according to a published protocol[11] and 25 $\mu$L of the casting solution was drop-cast onto 1 $cm^2$ Toray paper electrodes and allowed to dry overnight. For the DET bioanodes using fructose dehydrogenase (FDH), 50 $\mu$L of a 20 mg/mL enzyme solution in 50 mM citrate buffer (pH 4.5) was dropcast onto Toray carbon paper electrodes (area = 1 $cm^2$) and allowed to dry for 1 h. The electrodes were then soaked in 50 mM citrate buffer for an hour and rinsed with water to remove any loosely adsorbed enzyme.

**Table 1. Elemental Quantification of Unmodified and Anthracene-Modified MWCNTs Provided by XPS[a]**

| | C 1s % | O 1s % | C≡C | C═C | C−C |
|---|---|---|---|---|---|
| unmodified MWCNTs | 95.1 | 4.9 | 3.9 | 72.0 | 24.2 |
| anthracene-modified MWCNTs | 97.4 | 2.6 | 2.8 | 82.3 | 14.9 |

[a] Quantifications of carbon type are normalized with respect to the total amount of carbon−carbon bonds.

**Electrochemical Measurements.** Cyclic voltammetry experiments were carried out with a CH Instruments model 650A potentiostat (Austin, TX). Except for the fuel cell, all measurements were carried out with a traditional three-electrode setup consisting of a saturated calomel reference electrode (SCE) and a platinum mesh counter electrode in a buffer solution of 50 mM citrate, pH 4.5.

The fuel cell using the mediated glucose oxidase bioanode was an H-cell to keep the pH of the anodic and cathodic compartments different. The anodic compartment was filled with 50 mL of 50 mM sodium phosphate and 50 mM NaCl, and 60 mM glucose at pH 7.0. The cathodic compartment was filled with 50 mM citrate at pH 4.5. The membrane separating the two half-cells was a Nafion 212 proton exchange membrane. The fuel cell using the DET bioanode consisted of a single-compartment cell containing 50 mL of a quiescent solution of 50 mM citrate and 100 mM fructose at pH 4.5. The electrodes in this fuel cell were separated by a distance of ~1 cm. All biofuel cells were short-circuited 3 times, and the OCV was allowed to stabilize before polarization. Open circuit voltages and polarizations were measured with a Biologic VSP potentiostat/galvanostat or a Pine WaveNow potentiostat/galvanostat. All electrochemical measurements were carried out at 25 °C. Reported error and error bars correspond to one standard deviation.

## RESULTS AND DISCUSSION

**Anthracene-Modified MWCNTs.** Anthracene-modified MWCNTs (An-MWCNTs) were synthesized according to the procedure shown in Figure 1. To determine if the anthracene groups were attached to the MWCNTs, UV−vis and XPS were carried out on the modified MWCNTs. In the UV−vis experiment, the spectrum of 2-anthracenecarboxylic acid was used as a reference to compare to the spectrum of the modified MWCNTs. The spectrum of the An-MWCNTs was obtained by subtracting the spectrum of the unmodified −OH functionalized MWCNTs from that of the An-MWCNTs. As shown in Figure 2, the characteristic absorption peaks for the anthracene group between 315 and 400 nm are present in each spectrum,

showing that the anthracene groups are attached to the An-MWCNTs. The XPS data (shown in Table 1) shows an increase in the carbon to oxygen ratio in the modified MWCNTs and reveals a significant increase in the amount of $sp^2$ hybridized carbons (relative to other carbon hybridizations), giving strong evidence for the attachment of the anthracene groups onto the modified MWCNTs. While these experiments do not definitively prove that the anthracene groups are *covalently* attached at the hydroxylated sites on the MWCNTs, it is unlikely that a significant amount of anthracene groups would remain noncovalently attached to the MWCNTs after the extensive washing steps that were carried out after the reaction with anthracene-2-carbonyl chloride.

**Cyclic Voltammetry of Laccase/MWCNT Cathodes.** To evaluate the anthracene-modified MWCNTs as scaffolds for laccase-catalyzed DET oxygen reduction, cyclic voltammetry was carried out on biocathodes cast from An-MWCNTs, laccase, and TBAB-modified Nafion under various conditions. As shown in Figure 3, the covalent attachment of the anthracence groups on the MWCNTs resulted in the production of a catalytic $O_2$ reduction current at a sufficiently reducing potential. The control

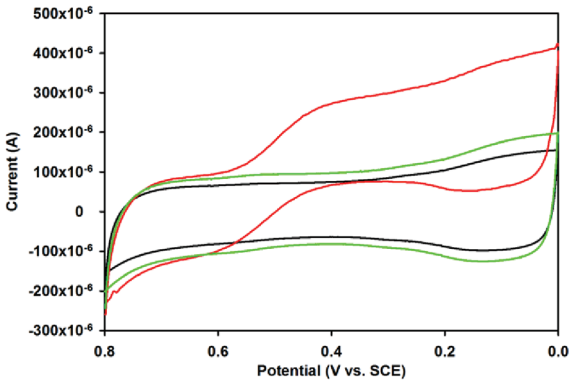


**Figure 3.** Cyclic voltammetry of laccase cathodes at 10 mV/s in pH 4.5 citrate buffer. Black is unmodified MWCNTs/laccase under air-saturated conditions, green is An-MWCNTs/laccase under $N_2$-saturated conditions, and red is An-MWCNTs/laccase under air-saturated conditions.

electrode, which consisted of laccase, TBAB-modified Nafion, and the unmodified −OH functionalized MWCNTs, did not produce any catalytic current, suggesting that laccase enzymes were not favorably oriented for DET with the unmodified MWCNTs. The CV for the An-MWCNT/laccase electrode under anaerobic conditions ($N_2$-saturated buffer) was similar to the one using unmodified MWCNTs, showing that the catalytic current generated in the air-saturated buffer was due to $O_2$ reduction. The background-subtracted catalytic current density obtained from the red CV in Figure 3 was 155 $\mu A/cm^2$, which is among the highest reported for nonrotating, two-dimensional DET enzymatic biocathodes in air- or oxygen-saturated solutions.[28,33,35,45,46] The catalytic current had an onset potential of 0.60 V versus SCE, which is near the reported redox potential of the T1 site of laccase from *Trametes versicolor*,[17] indicating an effective wiring of the laccase active sites to the modified nanotubes. A proposed scheme for how the anthracene groups direct the orientation of laccase enzymes is shown in Figure 4, with the hydrophobic pocket around the T1 active site of the enzyme oriented near the anthracene groups on the MWCNTs.

**Optimization of Laccase and An-MWCNT Loading.** To maximize the current production from these cathodes, the amounts of laccase and An-MWCNTs were optimized. Figure 5A shows a plot of current density versus An-MWCNT loading, obtained by mixing different amounts of An-MWCNTs with constant amounts of laccase and TBAB-modified Nafion and measuring the catalytic current density for each set of electrodes. At an An-MWCNT loading of 46 wt %, the catalytic current density was low, which is most likely due to low conductivity of the enzyme/nanotube/polymer matrix. Enough nanotubes must be loaded to eclipse the percolation threshold and create a fully conductive matrix. As the amount of An-MWCNTs increased, the catalytic current density increased, reaching a maximum at about 72 wt %. As the loading was increased further, the catalytic current density began to decrease, most likely because of limited oxygen diffusion into the polymer/nanotube matrix.

Once the An-MWCNT loading was optimized, the enzyme loading was varied, keeping all other parameters constant. As expected, electrodes with low enzyme loadings produced low currents, but the catalytic current density increased sharply as the amount of enzyme loading increased, with a maximum at about

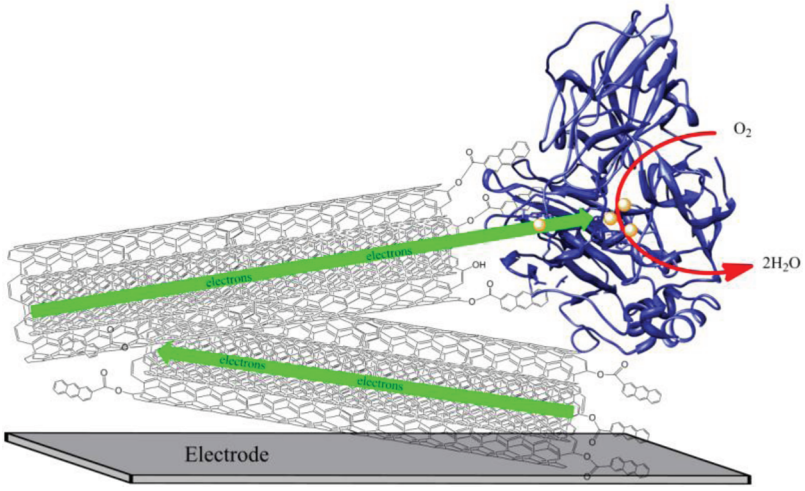


**Figure 4.** Idealized schematic of DET oxygen reduction by laccase, oriented with T1 site near anthracene groups.


dx.doi.org/10.1021/cs200475q |*ACS Catal.* 2011, 1, 1683–1690

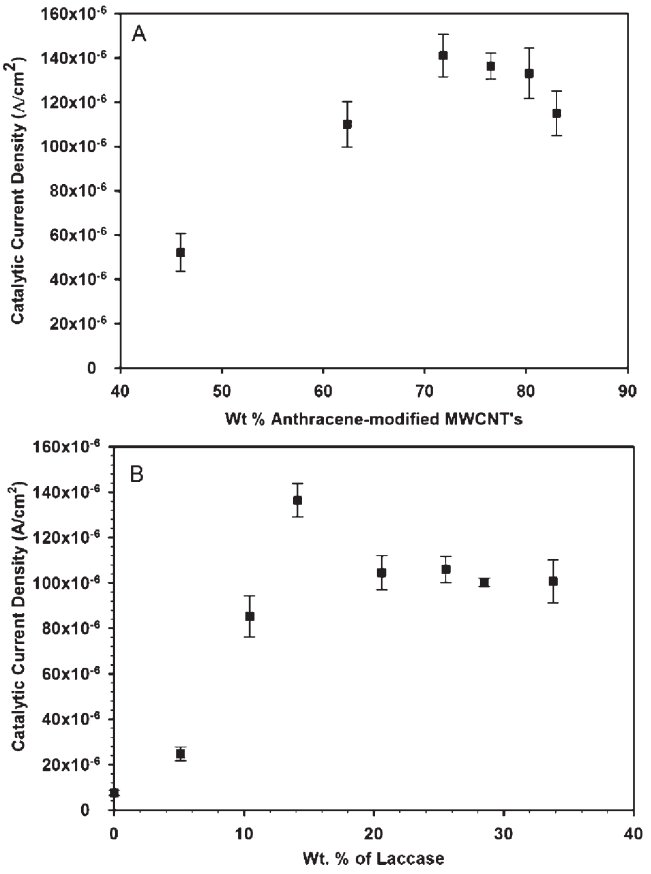


**Figure 5.** Optimization of An-MWCNT (A) and laccase (B) loading. Background-subtracted steady-state current densities of biocathodes made with varying amounts of laccase enzyme. Measurements taken in 50 mM citrate buffer, pH 4.5. All measurements made in triplicate; error bars correspond to 1 standard deviation.

14 wt % (Figure 5B). After this maximum, the catalytic current density dropped and enzyme loadings between 20 and 35% produced statistically similar current densities. This drop-off could be due to a lower electronic conductivity because of higher amounts of insulating protein mass intercalated within the conductive nanotube matrix. However, because the optimal laccase loading was only 14%, it is likely that other crude proteins in the commercial laccase slightly hindered the flow of electrons through the films, and we hypothesize that a purification of the laccase enzyme to remove crude protein mass could lead to improved current densities because of the ability to load more enzymatic protein mass into the conductive nanotube/polymer matrix. Future studies will focus on this hypothesis.

**Stability of the Biocathodes.** The low stability of enzymes and enzyme electrodes is one obstacle for the commercialization of biofuel cells, and the TBAB-modified Nafion polymer used in this study to immobilize the laccase and nanotubes has been shown to enhance the stability of immobilized enzymes.[16,47] As such, the stability of the cathodes was measured during constant operation and as a function of storage time. The operational stability of the biocathodes was investigated by both potentiostatic and galvanostatic methods, operating an electrode at either 0.3 V (vs SCE) for 24 h and measuring the current response, or at 100 $\mu$A for 24 h and measuring the voltage response. As shown in Figure 6, the biocathode that was poised at a constant potential

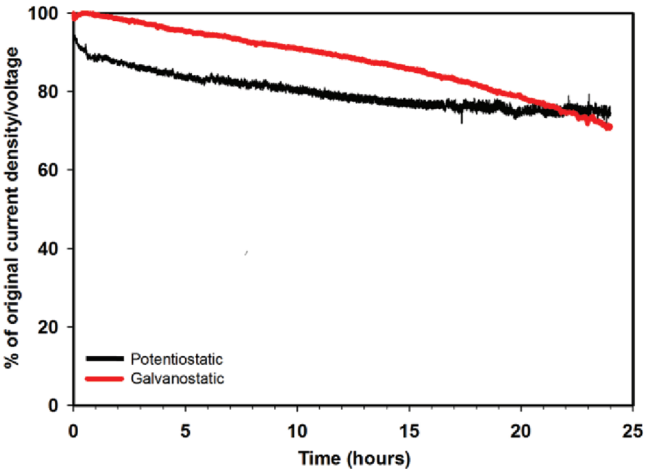


**Figure 6.** Operational stability of the cathode. Potentiostatic (black line): Cathode was poised at 0.3 V vs SCE in 50 mM citrate buffer, pH 4.5 at 25 °C for 24 h (air-saturated quiescent solution), and the current was measured as a function of time. Galvanostatic (red line): Under the same conditions, 100 $\mu$A of current was passed through the electrode for 24 h, and the voltage drop was measured as a function of time.

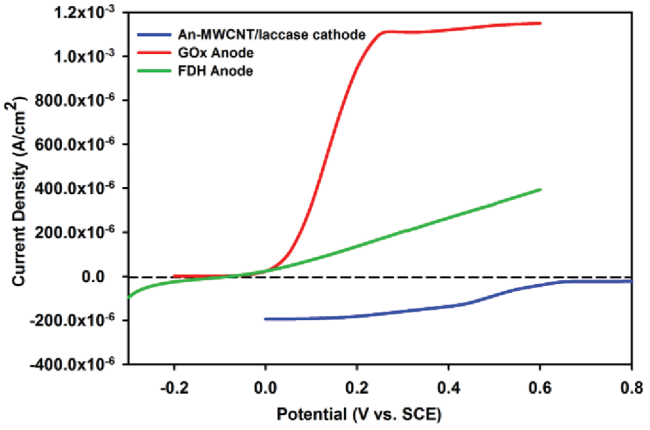


**Figure 7.** Half-cell polarization curves. Polarization of each electrode used in this study at 1 mV/s against an SCE reference. Dotted line through zero current is included for clarity. GOx anode: 50 mM phosphate, 50 mM NaCl, 80 mM glucose, pH 7.0. FDH anode: 50 mM citrate, 100 mM citrate, pH 4.5. An-MWCNT/laccase cathode: 50 mM citrate, pH 4.5.

was quite stable after an initial drop in current, retaining about 75% of its original current after 1 day of constant operation. While a 25% loss of original current density is significant, it is encouraging to note that most of the loss of performance occurred in the first 12 h. The cathode was very stable after that time period, with a current drop of only 4% from 12 to 24 h. The overall loss in galvanostatic stability was similar, with a voltage drop of 30% after continuous operation at 100 $\mu$A. However, this loss was almost linear in nature, and did not have an initial drop followed by high stability. The storage stability study revealed that the electrodes were stable when stored under refrigerated conditions, losing only 15% of their original catalytic current density after 1 month of storage at 4 °C. These losses in stability are curious given the high stability of biocathodes produced by Armstrong et al.,[36] and may suggest that electrodes constructed using enzyme/nanotube/polymer mixtures are less stable than those using the simple adsorption of enzymes.

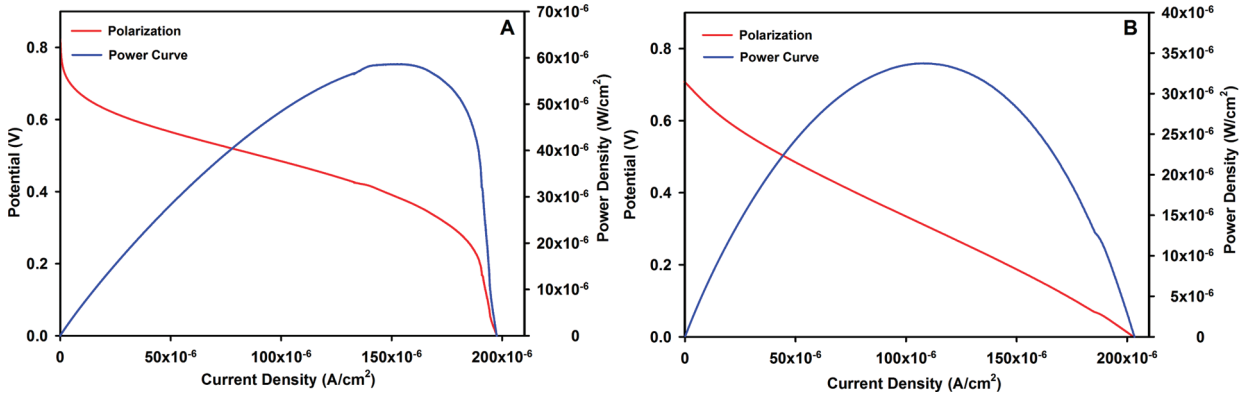


**Figure 8.** Enzymatic Biofuel Cells. Representative polarization and power curves of enzymatic biofuel cells consisting of an An-MWCNT/laccase/TBAB-Nafion biocathode and either a GOx/$FcMe_2$-$C_3$-LPEI bioanode (A) or a FDH bioanode (B). Electrodes were cast onto 1 $cm^2$ pieces of Toray paper. The glucose/$O_2$ fuel cell was a U-shaped cell with a Nafion 212 separator membrane, with the biocathode immersed in air-saturated 50 mM citrate buffer at pH 4.5, and the bioanode immersed in 50 mM sodium phosphate, 50 mM NaCl, 80 mM glucose, at pH 7.0. The fructose/$O_2$ fuel cell was a single compartment containing 50 mL of 50 mM citrate, 100 mM fructose, at pH 4.5.

**Enzymatic Biofuel Cell.** To test the performance of the DET biocathode in enzymatic biofuel cells, it was coupled to two different types of anodes. For the construction of a glucose/$O_2$ biofuel cell, a glucose oxidase (GOx) bioanode anode was used that utilized a dimethylferrocene-based redox polymer to wire the active sites of GOx to the electrode surface.[11] For a fructose/$O_2$ biofuel cell, a fructose dehydrogenase (FDH) bioanode was used, consisting of a layer of FDH adsorbed onto conductive carbon paper (for further characterization of the performance and stability of this anode, see the Supporting Information, Figures S1 and S2). Each bioanode had the same geometric area as the biocathode (1 $cm^2$), and polarizations of each electrode (Figure 7) revealed that both bioanodes were able to produce higher currents than the biocathode, meaning that the biocathodes were limiting in each type of biofuel cell studied.

To construct the glucose/$O_2$ biofuel cell, an H-Cell was used to keep each electrode near its optimal pH (7.0 for GOx and 4.5 for laccase). A Nafion 212 proton exchange membrane was placed between each half-cell to separate the solutions. Representative polarization and power curves for this biofuel cell are shown in Figure 8A. Because the mediator used in the GOx anode had a relatively low redox potential for a ferrocene-based redox polymer ($E_{1/2}$ = 0.41 V vs NHE),[11] the biofuel cell produced a high open circuit voltage of 0.819 ± 0.022 V. When the cell was polarized, it produced a maximum power density of 56.8 (±1.8) $\mu$W/$cm^2$ and a maximum current density of 205.7 (±7.8) $\mu$A/$cm^2$. The maximum power density occurred at 0.410 ± 0.019 V, which is approximately the difference between the redox potentials of laccase and the redox polymer (0.82 and 0.41 V vs NHE, respectively).[11,17] This potential at maximum power is more than twice the voltage produced at maximum power when a mediated biocathode was coupled with the anodic redox polymer and near to 0.5 V, at which a simple three-cell stack could be fabricated to power small electronic devices (a typical calculator or small flashlight can operate using a coin-cell battery with a discharge potential of 1.5 V).

The use of FDH as a bioanode allowed for the construction of a compartment-less biofuel cell as FDH is oxygen tolerant and has a pH optimum between pH 4 and 5, similar to laccase. In addition, laccase can operate efficiently in the presence of a variety of biofuels, and the biocathodes in this study showed no drop in performance with the addition of fructose (data not shown). FDH is in the quinohemoprotein family of enzymes and has a pyrroloquinoline quinone (PQQ) cofactor that is used for substrate oxidation. Following substrate oxidation, electrons are passed to heme groups which can communicate directly with an electrode surface, and a variety of electrodes have been utilized to facilitate DET from the FDH enzyme.[30,32,48−50] Most of these anodes use some type of high surface-area conductive matrix in which to immobilize FDH.

We found that simply adsorbing FDH onto conductive carbon paper produced DET bioanodes with limiting current densities above 300 $\mu$A/$cm^2$ (Figure 7 and Supporting Information, Figure S1). Unlike the polarization of the mediated GOx bioanode that reached a steady-state at ∼0.25 V (vs SCE), the current from the FDH bioanodes increased linearly with potential. This is likely due to nondiffusion controlled bioelectrocatalysis, a behavior that has been shown before in other FDH anodes using DET.[32,51,52] The FDH bioanode was coupled to the biocathode to create a compartment-less biofuel cell using only direct bioelectrocatalysis (Figure 8B). This DET biofuel cell produced an OCV of 0.707 ± 0.005 V, which is about 100 mV less than the OCV of the biofuel cell with the mediated bioanode. This lower OCV of the DET cell is surprising in light of the similar onset of fuel oxidation for each bioanode, which occurs at ∼0.03 V (Figure 7) and is likely due to less of a pH gradient than was present in the compartmentalized cell. When the fructose/$O_2$ biofuel cell was polarized, it produced a maximum current density of 201.7 (±14.4) $\mu$A/$cm^2$ and a power density of 34.4 (±2.7) $\mu$W/$cm^2$ at 0.329 ± 0.004 V. The maximum current density of the DET biofuel cell was not statistically different from that of the biofuel cell with the mediated bioanode, so it was surprising that the maximum power density was ∼40% lower. As the onset potentials for fuel oxidation at each anode are identical and the maximum current densities produced in each cell are similar, it is probable that the higher power density of the compartmentalized cell is due to the presence of the pH gradient, which provides an additional source of potential energy in that cell and thus higher power density as well.

## ■ CONCLUSIONS

Multiwalled carbon nanotubes were covalently modified with anthracene groups to facilitate the favorable orientation of the

active site of laccase near the MWCNT surface, enabling facile direct electron transfer from the An-MWCNTs to the T1 copper atom of the enzyme. Catalytic current densities resulting from bioelectrocatalytic $O_2$ reduction with this system are among the highest reported for systems where a MCO is physically mixed or adsorbed onto a conductive matrix. (A few recent studies have recently reported DET current densities for enzymatic $O_2$ reduction well above 1 mA/cm$^2$, but these studies utilized other methods of enzyme entrapment such as liquid-induced shrinkage[30] or high pressures.[31])

After optimizing the various parameters of the biocathode, it was utilized in two different types of biofuel cells: a biofuel cell with a mediated GOx anode and a biofuel cell with a DET FDH anode. The use of the mediated bioanode required the use of a compartmentalized cell while the use of FDH allowed for a simple electrode fabrication process and removed the need for separate compartments for each electrode, resulting in a simpler cell construction. The onset for fructose oxidation at the FDH bioanode was similar to the onset for glucose oxidation at the GOx anode and each bioanode was able to produce more current than the biocathode, but the performance of the biofuel cell with the mediated bioanode was superior. This superior performance is attributed to an additional source of potential energy from a pH gradient between the electrodes in the compartmentalized cell.

Using the maximum current density produced by the biofuel cells, the units of enzyme present on each electrode (~3.6 Units, calculated by weight subtraction after casting of the enzyme/nanotube/polymer mixture), and the activity of the enzyme (20 Units/mg), it was found the biocathode produced only ~2% of the theoretical maximum current density, indicating that many of the laccase enzymes are either denatured or not electrically connected to the electrode surface despite the presence of the anthracene groups. Future studies will focus on increasing this efficiency by alternative nanotube modifications and/or the investigation of other immobilization polymers.

## ■ ASSOCIATED CONTENT

**Supporting Information.** Characterization data for the FDH bioanode is given in Figures S1 and S2 together with a discussion of this data. This material is available free of charge via the Internet at http://pubs.acs.org.

## ■ AUTHOR INFORMATION

### Corresponding Author

*E-mail: minteer@chem.utah.edu.

### Funding Sources

M.T.M and S.D.M would like to thank the United Soybean Board, National Science Foundation, and the Air Force Office of Scientific Research for funding this work. D.H. and D.T.G. would like to thank the National Science Foundation and the Oklahoma Bioenergy Center for support.

## ■ REFERENCES

(1) Cracknell, J. A.; Vincent, K. A.; Armstrong, F. A. *Chem. Rev.* **2008**, *108*, 2439.
(2) Kim, J.; Jia, H.; Wang, P. *Biotechnol. Adv.* **2006**, *24*, 296.
(3) Calabrese-Barton, S.; Gallaway, J.; Atanassov, P. *Chem. Rev.* **2004**, *104*, 4867.
(4) Sarma, A. K.; Vatsyayan, P.; Goswami, P.; Minteer, S. D. *Biosens. Bioelectron.* **2009**, *24*, 2312.
(5) Kavanagh, P.; Boland, S.; Jenkins, P.; Leech, D. *Fuel Cells* **2009**, *9*, 79.
(6) Liu, D.; Liu, H.; Hu, N. *Electrochim. Acta* **2010**, *55*, 6426.
(7) Schlapfe, P.; Mindt, W.; Racine, P. *Clin. Chim. Acta* **1974**, *57*, 283.
(8) Meredith, M. T.; Minteer, S. D. *Anal. Chem.* **2011**, *83*, 5436.
(9) Mao, F.; Mano, N.; Heller, A. *J. Am. Chem. Soc.* **2003**, *125*, 4951.
(10) Heller, A. *Curr. Opin. Chem. Biol.* **2006**, *10*, 664.
(11) Meredith, M. T.; Glatzhofer, D.; Kao, D.-Y.; Schmidtke, D. W.; Hickey, D. *J. Electrochem. Soc.* **2011**, *158*, B166.
(12) Bunte, C.; Prucker, O.; Konig, T.; Ruhe, J. *Langmuir* **2010**, *26*, 6019.
(13) Stoica, L.; Dimcheva, N.; Ackermann, Y.; Karnicka, K.; Guschin, D. A.; Kulesza, P. J.; Rogalski, J.; Haltrich, D.; Ludwig, R.; Gorton, L.; Schuhmann, W. *Fuel Cells* **2009**, *9*, 53.
(14) Arechederra, M. N.; Addo, P. K.; Minteer, S. D. *Electrochim. Acta* **2011**, *56*, 1585.
(15) Sokic-Lazic, D.; Minteer, S. D. *Biosens. Bioelectron.* **2008**, *24*, 939.
(16) Akers, N. L.; Moore, C. M.; Minteer, S. D. *Electrochim. Acta* **2005**, *50*, 2521.
(17) Gallaway, J. W.; Barton, S. A. C. *J. Am. Chem. Soc.* **2008**, *130*, 8527.
(18) Hecht, H. J.; Kalisz, H. M.; Hendle, J.; Schmid, R. D.; Schomburg, D. *J. Mol. Biol.* **1993**, *229*, 153.
(19) Arechederra, R. L.; Minteer, S. D. *Fuel Cells* **2009**, *9*, 63.
(20) Tasca, F.; Gorton, L.; Harreither, W.; Haltrich, D.; Ludwig, R.; Noll, G. *J. Phys. Chem. C* **2008**, *112*, 9956.
(21) Tasca, F.; Harreither, W.; Ludwig, R.; Gooding, J. J.; Gorton, L. *Anal. Chem.* **2011**, *83*, 3042.
(22) Quintanar, L.; Stoj, C.; Taylor, A. B.; Hart, P. J.; Kosman, D. J.; Solomon, E. I. *Acc. Chem. Res.* **2007**, *40*, 445.
(23) Hakulinen, N.; Kiiskinen, L. L.; Kruus, K.; Saloheimo, M.; Paananen, A.; Koivula, A.; Rouvinen, J. *Nat. Struct. Biol.* **2002**, *9*, 601.
(24) Solomon, E. I.; Sundaram, U. M.; Machonkin, T. E. *Chem. Rev.* **1996**, *96*, 2563.
(25) Léger, C.; Bertrand, P. *Chem. Rev.* **2008**, *108*, 2379.
(26) Kamitaka, Y.; Tsujimura, S.; Setoyama, N.; Kajino, T.; Kano, K. *Phys. Chem. Chem. Phys.* **2007**, *9*, 1793.
(27) Ivnitski, D.; Atanassov, P. *Electroanalysis* **2007**, *19*, 2307.
(28) Rubenwolfa, S.; Strohmeiera, O.; Kloke, A.; Kerzenmacher, S.; Zengerle, R.; Stetten, F. v. *Biosens. Bioelectron.* **2010**, *26*, 841.
(29) Flexer, V.; Brun, N.; Courjean, O.; Backov, R.; Mano, N. *Energy Environ. Sci.* **2011**, *4*, 2097.
(30) Miyake, T.; Yoshino, S.; Yamada, T.; Hata, K.; Nishizawa, M. *J. Am. Chem. Soc.* **2011**, *133*, 5129.
(31) Zebda, A.; Gondran, C.; Goff, A. L.; Holzinger, M.; Cinquin, P.; Cosnier, S. *Nat. Commun.* **2011**, *2*, 1.
(32) Kamitaka, Y.; Tsujimura, S.; Setoyama, N.; Kajino, T.; Kano, K. *Phys. Chem. Chem. Phys.* **2007**, *9*, 1793.
(33) Ramasamy, R. P.; Luckarift, H. R.; Ivnitski, D. M.; Atanassov, P. B.; Johnson, G. R. *Chem. Commun. (Cambridge, U. K.)* **2010**, *46*, 6045.
(34) Pang, H. L.; Liu, J.; Hu, D.; Zhang, X. H.; Chen, J. H. *Electrochim. Acta* **2010**, *55*, 6611.
(35) Thorum, M. S.; Anderson, C. A.; Hatch, J. J.; Campbell, A. S.; Marshall, N. M.; Zimmerman, S. C.; Lu, Y.; Gewirth, A. A. *J. Phys. Chem. Lett.* **2010**, *1*, 2251.
(36) Blanford, C. F.; Foster, C. E.; Heath, R. S.; Armstrong, F. A. *Faraday Discuss.* **2009**, *140*, 319.
(37) Blanford, C. F.; Heath, R. S.; Armstrong, F. A. *Chem. Commun. (Cambridge, U. K.)* **2007**, *17*, 1710.
(38) Pita, M.; Gutierrez-Sanchez, C.; Olea, D.; Velez, M.; Garcia-Diego, C.; Shleev, S.; Fernandez, V. M.; Lacey, A. L. D. *J. Phys. Chem. C* **2011**, *115*, 13420.
(39) Martinez-Ortiz, J.; Flores, R.; Vazquez-Duhalt, R. *Biosens. Bioelectron.* **2011**, *26*, 2626.
(40) Schubert, K.; Goebel, G.; Lisdat, F. *Electrochim. Acta* **2009**, *54*, 3033.

(41) Santos, L. d.; Climent, V.; Blanford, C. F.; Armstrong, F. A. *Phys. Chem. Chem. Phys.* **2010**, *12*, 13962.
(42) Klotzbach, T.; Watt, M.; Ansari, Y.; Minteer, S. D. *J. Membr. Sci.* **2006**, *282*, 276.
(43) Dawn, A.; Shiraki, T.; Haraguchi, S.; Sato, H.; Sada, K.; Shinkai, S. *Chem.—Eur. J.* **2010**, *16*, 3676.
(44) Lin, Y.-c.; Kachar, B.; Weiss, R. G. *J. Am. Chem. Soc.* **1989**, *111*, 5542.
(45) Zheng, W.; Zho, H. M.; Zheng, Y. F.; Wang, N. *Chem. Phys. Lett.* **2008**, *457*, 381.
(46) Habriouxa, A.; Napporna, T.; Servat, K.; Tingry, S.; Kokoh, K. B. *Electrochim. Acta* **2010**, *55*, 7701.
(47) Moore, C. M.; Akers, N. L.; Hill, A. D.; Johnson, Z. C.; Minteer, S. D. *Biomacromolecules* **2004**, *5*, 1241.
(48) Tkac, J.; Svitel, J.; Vostiar, I.; Navratil, M.; Gemeiner, P. *Bioelectrochemistry* **2009**, *76*, 53.
(49) Ramanavicius, A.; Ramanaviciene, A. *Fuel Cells* **2009**, *9*, 25.
(50) Murata, K.; Kajiya, K.; Nakamura, N.; Ohno, H. *Energy Environ. Sci.* **2009**, *2*, 1280.
(51) Kamitaka, Y.; Tsujimura, S.; Kano, K. *Chem. Lett.* **2007**, *36*, 218.
(52) Murata, K.; Suzuki, M.; Kajiya, K.; Nakamura, N.; Ohno, H. *Electrochem. Commun.* **2009**, *11*, 668.